Applied Nanoscience (2023) 13:7477–7483
https://doi.org/10.1007/s13204-023-02927-x

ORIGINAL ARTICLE

# Structure and properties of biogenic hydroxyapatite bioceramics modified by graphene-like structures

A. Iatsenko[1] · O. Sych[2,3] · A. Synytsia[2] · P. Zaremba[4] · S. Zahorodnia[4] · A. Nikolenko[5] · T. Tomila[2] · O. Bykov[2]

Received: 16 December 2022 / Accepted: 4 July 2023 / Published online: 29 July 2023


## Abstract

Today bone tissue engineering is one of the most used technologies for treat bones injure. Materials containing hydroxyapatite and graphene have received much attention recently. The aim of this study was preparation of biogenic hydroxyapatite bioceramics modified by graphene-like structures investigation effect of graphene on the structure and properties of material. Biogenic hydroxyapatite bioceramics modified by graphene-like structures were successfully prepared by chemical vapor deposition (CVD) method. Subsequently, microstructure, composition, specific surface area, skeleton density, resorption rate in physiological solution and cytotoxicity were evaluated. XRD, IR spectroscopy, micro-Raman spectroscopy and SEM proved graphene oxide's formation on biogenic hydroxyapatite as well as on silica single crystal for comparison. Although the coating of graphene-like structures on biogenic hydroxyapatite bioceramics reduces the specific surface area, it allows to 4 times increase resorption rate of biogenic hydroxyapatite bioceramics in physiological solution and does not affect the overall assessment of the cytotoxicity. MTT assay established non-cytotoxic effect and indicated a high potential of biogenic hydroxyapatite bioceramics modified by graphene-like structures using CVD method for medical application.

**Keywords** Hydroxyapatite · Graphene · Chemical-vapor deposition method · Biomaterial · Cytotoxicity

## Introduction

For many years, hydroxyapatite (synthetic and biogenic) as an analogue of inorganic component of natural bone has been a leader due to its similarity to natural bone tissue and high biocompatibility (Heise et al. 1990; Hench and Jones 2005; Kattimani et al. 2016; Shi et al. 2021). Biogenic hydroxyapatite (BHA) that has perfect bioactivity and allows reducing the cost of the finished implant material is currently obtained from cattle bones, shells of mollusks, cuttlefish, sea corals and algae, eggshells (Sadat-Shojai et al. 2013; Arokiasamy et al. 2022). In our previous work (Sych et al. 2007; Sych and Pinchuk 2007; Tovstonog et al. 2015), it was shown that the BHA powder prepared by calcination of bovine bone was composed of irregularly formed agglomerates from round 100–500 nm particles, contains in its composition only hydroxyapatite phase as well as after microwave and conventional sintering at temperature 1100 °C. BHA was also used for preparation of different modified composites and found the significant increase in osteogenic activity of bone marrow stromal stem cells of human ilium outside the local foci of inflammation and degenerative lesions in the presence BHA ceramics and highly porous glass ceramics based on BHA (Panchenko et al. 2014; Sych 2015; Tovstonoh et al. 2016; Sych et al. 2015, 2016, 2017; 2018a, b).

✉ O. Sych
lena_sych@ukr.net

1 Department of Chemical Technology of Ceramics and Glass, National Technical University of Ukraine "Igor Sikorsky Kyiv Polytechnic Institute", Peremogy Ave., 37, Kyiv 03056, Ukraine

2 Frantsevich Institute for Problems of Materials Science, NAS of Ukraine, 3 Omeliana Pritsaka (Krzhyzhanovsky) Str., Kyiv 03142, Ukraine

3 Laboratory of Nanostructures, Institute of High Pressure Physics "Unipress", PAS, 01-142 Warsaw, Poland

4 Department of Reproduction Virus, D. Zabolotny Institute of Microbiology and Virology, NAS of Ukraine, 154 Akademika Zabolotny Str., Kyiv 03143, Ukraine

5 Laboratory of Optical Submicron Spectroscopy, Institute of Semiconductor Physics NAS of Ukraine, 45 Nauky Ave, Kyiv 03028, Ukraine

Significant interest in recent years to medical application of graphene and graphene-like (such as graphene oxide) structures is associated with their unique optical, electrical, chemical properties and structure and possibility to use as diagnosing cancer, targeted drug delivery, photothermal therapy and tissue engineering (Zhang et al. 2012; Zhang et al. 2022).

A special place among the unique applications of graphene belongs to tissue engineering, including bone tissue engineering, due to its ability to accelerate the growth, differentiation and proliferation of stem cells. In addition, research on the antibacterial effect of graphene nanosheets has shown that graphene oxide can be used as a surface coating material for implants (Li et al. 2018; Ghosal et al. 2021). Graphene-like fabrication methods involve top-down (mechanical exfoliation, liquid phase exfoliation, electrochemical exfoliation, reduction of graphite oxide) and bottom-up (chemical vapor deposition (CVD), laser-assisted synthesis, epitaxial growth, pyrolysis production, organic synthesis and carbon monoxide reduction) approaches (Zhang et al. 2012; Li et al. 2018). One of the simplest, cheapest and scalable ways to obtain a graphene-like coating on is CVD method. Moreover, it allows to cover materials different size and form.

That is why the aim of the present work was preparation of biogenic hydroxyapatite ceramics modified by graphene-like structures by CVD method and study effect of graphene on the structure and properties of bioceramics.

## Materials and methods

### Materials

The starting material was biogenic hydroxyapatite (BHA) with particle size less 160 μm obtained from bovine bone by calcination at 800 °C and silicon single crystal (Si).

### Preparation of BHA and BHA-GO bioceramics

BHA was used for modification by graphene-like structures (BHA-GO) as a powder or compacted ceramics. Compacted samples with diameter of 15 mm and height 10 mm were obtained by uniaxial pressing at 50 MPa. Modification by graphene-like structures of BHA (BHA-GO) was conducted by chemical vapor deposition (CVD) method that is based on the chemical thermal decomposition of a precursor, so their individual constituents can build up a solid film or nanostructure into a specified substrate.

Figure 1 presents scheme for samples coating by CVD method. Experimental samples and catalyst (thin copper tape) were loaded in a quartz tube vacuum furnace followed by sealing the working space to a residual pressure ≤ 0.1 kPa with subsequent inletting of inert gas to pressure 100 kPa. Then, the working space was pumping with simultaneous heating up to 600 ℃ with duration of 30 min followed by inletting of LPG to a residual pressure of 50 kPa with rate of 1 kPa/s and turning off heating and cooling down to temperature ≤ 50 ℃. The last stage is inlet air, depressurizing the working space of the furnace and removing experimental samples. For comparison, Si were coated by graphene-like structures by the same method (Si-GO) too. Figure 1 presents scheme for samples coating by CVD method.

### Characterization

The microstructure was investigated by scanning electron microscopy using a Tescan Mira 3 LMU microscope (Tescan, Czech Republic).

XRD patterns were collected for BHA and BHA-GO powders on an DRON-3 X-ray diffractometer

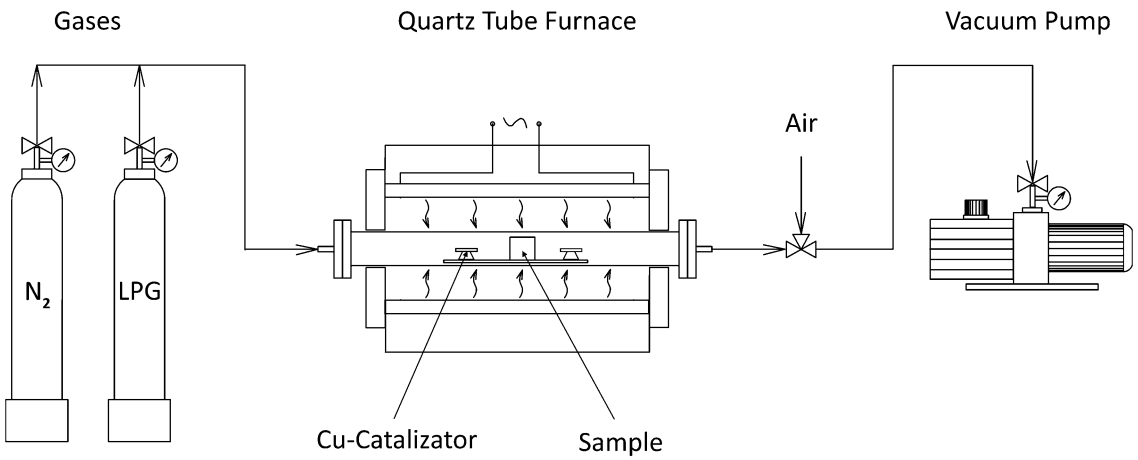


**Fig. 1** Scheme for samples coating by CVD method

(Bourevestnik, Russia) using Cu-Kα radiation with $\lambda = 1{,}54{,}178$ Å$^3$. For clearer results, Si and Si-GO were used for XRD characterization too.

IR spectra were recorded from 400 to 4000 cm$^{-1}$ using KBr pellets technology (investigated powder material was mixed with KBr powder at a ratio of 1:300 mg and pressed into transparent round tablets with a diameter of 13 mm) by Fourier-spectrometer FCM 1202 (Infraspectr, Russia).

Specific surface area was measured by analysis of the BET isotherm method using a Gemini 2360 instrument by Micromeritics according to ISO 9277:2010.

The density was measured using a helium pycnometer (AccuPyc II 1340, Micromeritics) at 24 ± 2 °C, according to ISO 12154:2014.

Before the density and specific surface area measurements were carried out, materials were dried at 150 °C for 2 h in vacuum (VacPrep 061 Sample Degas System by Micromeritics).

The micro-Raman measurements were conducted at room temperature in backscattering geometry using a Horiba Jobin Yvon T-64000 Raman spectrometer fitted with an Olympus BX41 microscope. A line of Ar–Kr ion laser with a wavelength of 488 nm was used for excitation. The laser beam was directed onto the sample surface with a 50×/NA 0.75 objective, producing a spot approximately 1 µm in diameter. The laser power applied to the sample surface was limited to less than 1 mW to prevent structural damage or heating.

Experiments in vitro (resorption rate) of composite were conducted at static conditions in physiological solution (saline, 0.9% NaCl aqueous solution), which is an isotonic solution of body fluids and is one of the most often used to dissolve various drugs and injections. Compacted disk shape samples with porosity ~ 43% were used for investigation. Previously, the samples were dried in drying cabinet at 100 °C for 2 h, weighed by an analytical balance "OHAUS Pioneer PA214C" (OHAUS Corporation, China) and immersed in saline (solid phase/liquid phase = 1:50). A constant temperature of 36.5 ± 0.5 °C was maintained by TS-1/80 SPU thermostat (Smolenskoe SKTB SPU OAO, Russia). After 48 h, samples were thoroughly washed with distilled water, dried and weighed. The resorption rate of composite materials was determined as a specific mass loss during the experimental time. The chemical composition of physiological solution after maintaining of samples was analyzed by energy-dispersive X-ray fluorescence elemental analysis (Expert 3L Analyzer, INAM, Ukraine). Data were represented as mean ± standard deviation of three to five independent experiments.

Cytotoxicity was studied as cell viability using MTT assay based mainly on the activity of dehydrogenases in mitochondria, which can convert 3,(4,5-dymetyltriazol-2-yl)-2,5-dyfeniltetrazolium bromide (MTT) to formazan. The conversion of MTT to formazan decreases with cell death and under an influence of toxic substances. MTT substrate ("Sigma," USA) was dissolved in sterile phosphate buffer (pH 7.2) at room temperature to a concentration of 5 mg/ml. The materials diluted in the growth media were added (200 µl per well) to 96-well plates with cell monolayer (MDCK—Madin–Darby canine kidney cells) and incubated for 48 h at 37 °C and 5% of $CO_2$. After that 20 µl of MTT solution was added to the wells and incubated at 37 °C for 2.5–4 h. Then, growth media was removed and 150 µl of 96% ethanol was added to dissolve the formazan crystals. The optical density of solutions was determined by Multiscan FC spectrophotometer (Thermo Fisher Scientific, USA) at wavelength of 538 nm. Percentage of cell viability was determined according to quantity of formazan that was synthetized in the experimental samples and compared with the control ones:

$$\text{Cell viability}[\%] = 100 \times \left(\frac{A}{B}\right),$$

where $A$ is the average value of the optical density for experimental samples, $B$ is the average value of the optical density for control samples.

Data were represented as mean ± standard deviation of three to five independent experiments. ANOVA was employed for the statistical evaluation of data, and $p < 0.05$ was deemed to be significant.

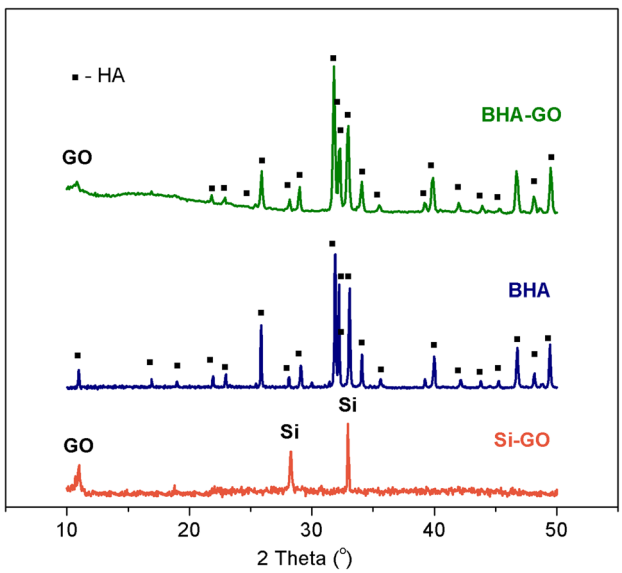


**Fig. 2** XRD patterns for BHA, BHA-GO and Si-GO

## Results and discussions

Figure 2 lists the XRD patterns for staring BHA, BHA-GO (BHA modified by graphene-like structures) and silicon single crystal modified by graphene-like structures (Si-GO) in range $2\theta$ from 10 to 50° that is the most important and illustrative. XRD data showed formation GO layer on BHA and silicon single crystals (peak at ~ 11°) that (Türk et al. 2018; Chandra Sekhar Boyapati et al. 2022). As seen, the graphene peak is low, unclear and overlap that could be connected with the low content of graphene oxide in comparison with hydroxyapatite (HA, $Ca_5(PO_4)_3OH$, PDF No. 9-0432) and silicon (Si, PDF No. 79-0613).

Figure 3 presents IR spectra of starting BHA and BHA modified by graphene-like structures. The analysis of the data showed that both samples are characterized by a set of absorption bands that characterize crystalline hydroxyapatite phase related to the vibrations of $PO_4^{3-}$ (1090, 1050, 960, 604, 570 and 470 $cm^{-1}$) and $OH^-$ (3570, 3440, 1630, 630 $cm^{-1}$) groups. In addition, the spectrum reflexes the vibrations of the carbonate group (1550, 1457, 1415, 880, 800 $cm^{-1}$) and $CO_3^{2-}$ ions are located in both the A-site (replacing $OH^-$ groups) and the B-site (replacing $PO_4^{3-}$ groups). The spectra of BHA and BHA-GO differ only in the intensity of the absorption bands. The decrease in the intensity of all IR bands for the BGA-GO sample shows that there is a coating of particles with graphene oxide that is also confirmed by BET results and decrease in the specific surface area after coating (Table 1).

The Raman spectrum from the silicon single crystal coated by graphene-like structures is shown in Fig. 4. The spectrum presents D and G peaks (~ 1345 and ~ 1600 $cm^{-1}$, respectively), and wide splitting of 2D bands centered at ~ 2900 $cm^{-1}$ that connected with graphene oxide and agree very well with other reports (Slobodian et al. 2018; Kaniyoor and Ramaprabhu 2012; Claramunt et al. 2015).

Figure 5 lists microstructure of starting BHA, BHA modified by graphene-like structures BHA-GO and silicon single crystals coated by graphene-like structures Si-GO. SEM images showed formation similar multilayer graphene-like on the surface of BHA and silicon single crystals.

Figure 6 presents nitrogen adsorption linear plot and BET surface area plot for BHA and BHA-GO powder. According to obtained results, both powders can be characterized as microporous materials, because isotherm shape belongs to type I isotherms according to the IUPAC classification (McNaught and Wilkinson 2019; Gregg and Sing 1982). The BET curve has a linear character and its linear region is shifted toward lower relative pressures, which is known to be characteristic of microporous materials. According to the

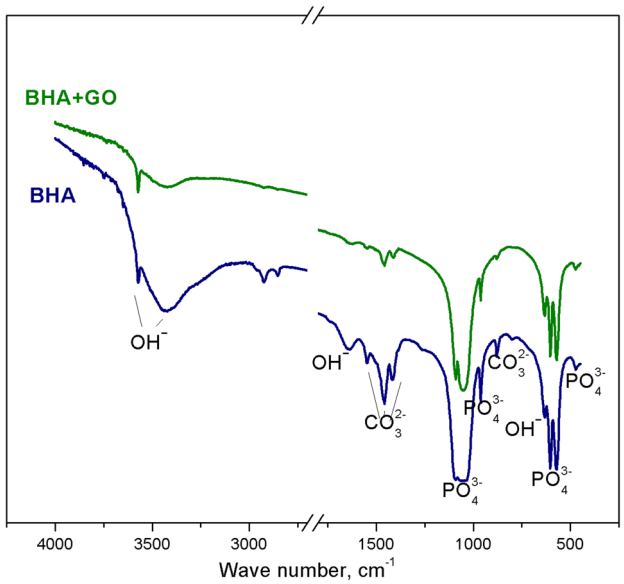


**Fig. 3** IR spectra for BHA and BHA-GO

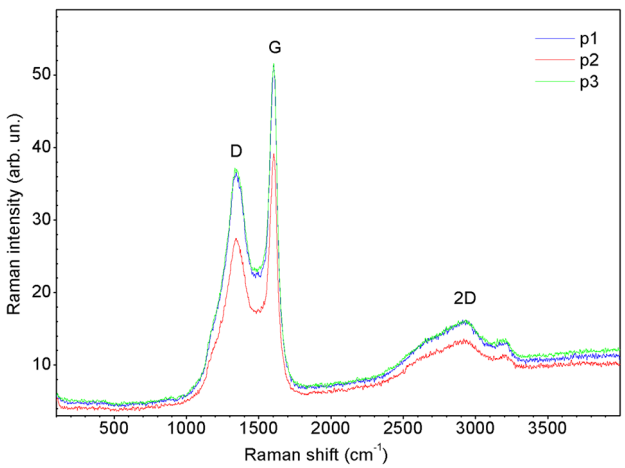


**Fig. 4** Raman spectra for Si-GO

**Table 1** Properties of BHA and BHA-GO

| Material | Specific surface area, $m^2/g$ | | | Skeleton density, $g/cm^3$ | Resorption rate, % wt./day |
|---|---|---|---|---|---|
| | BET multi-point | BET single point | Langmuir | | |
| BHA | 4.4 | 4.5 | 6.7 | 3.09 ± 0.01 | 0.18 (Sych 2015) |
| BHA–GO | 3.1 | 2.9 | 5.1 | 3.06 ± 0,01 | 0.81 |

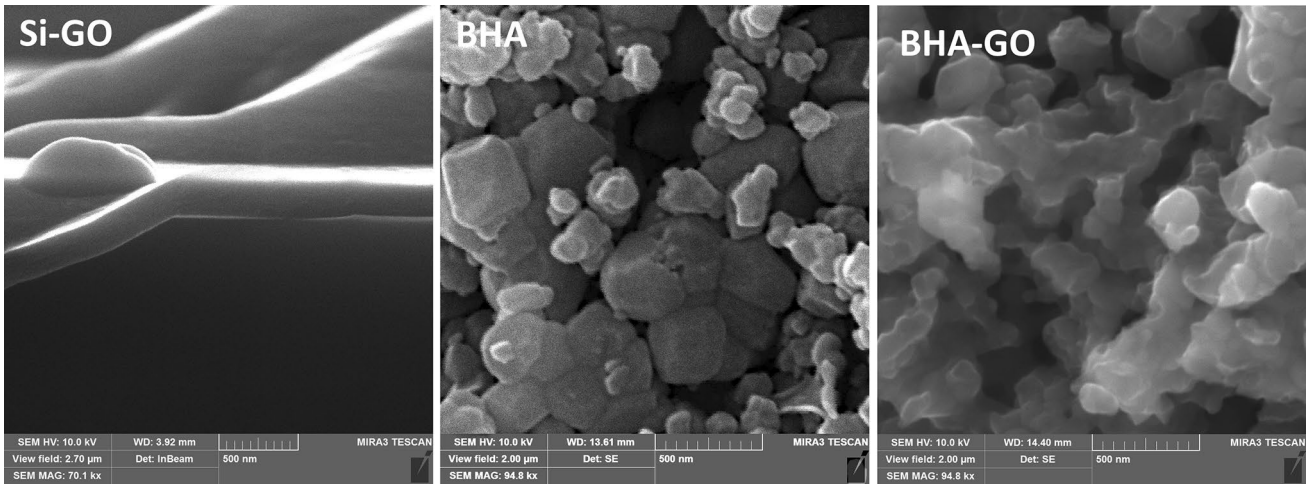


**Fig. 5** SEM for BHA, BHA-GO and Si-GO

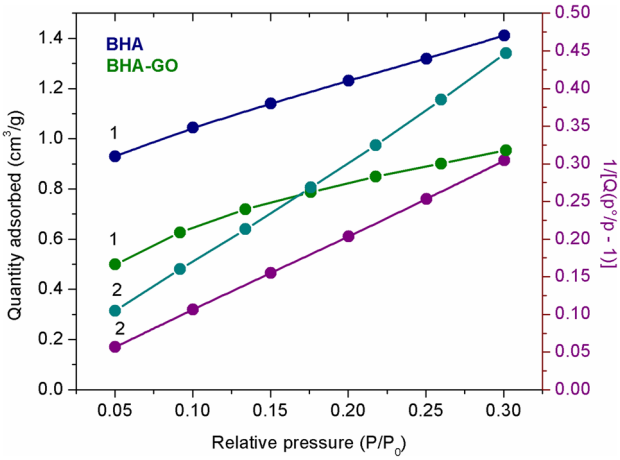


**Fig. 6** Nitrogen adsorption isotherm linear plot (1) and BET surface area plot (2) for BHA and BHA-GO

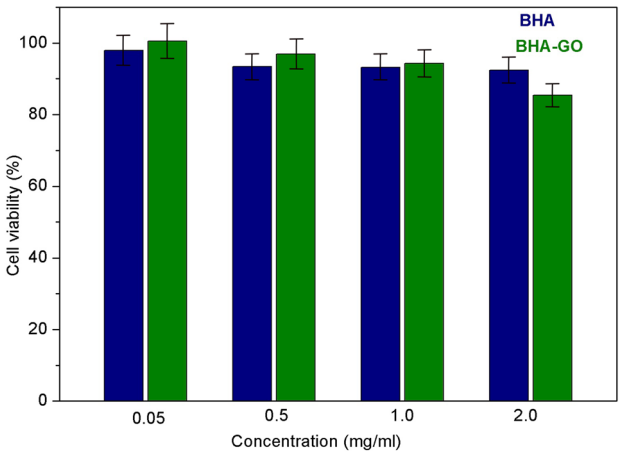


**Fig. 7** Cytotoxic effect of BHA and BHA-GO on MDKC cells

obtained results, modification BHA by graphene-like structures turns to decrease specific surface area. At the same time, it allows to 4 times increase resorption rate of BHA bioceramics in physiological solution that could be useful for creation of biomaterials. The energy-dispersive X-ray fluorescence elemental analysis showed that physiological solution after resorption rate investigations contains 0.004 and 0.010% of Ca for BHA and BHA-GO, respectively, which confirms the increase in solubility after coating. In addition, there was not found a significant effect of graphene-like coating on the skeleton density of materials, only a slight decrease, which was $3.09 \pm 0.01$ g/cm$^3$ and $3.06 \pm 0.01$ g/cm$^3$, for BGA and BGA-GO, respectively.

Figure 7 shows the results to determine the cytotoxic effect of BHA and BHA modified by graphene-like structures on MDCK cells obtained by MTT assay. As can be seen, in the concentration range of 0.05–2 mg/ml, both materials do not have a cytotoxic effect, since the percentage of cell viability is more than 85%. Although the coating of graphene-like structures on BHA at the maximum studied concentration slightly reduced the viable cell population, this does not affect the overall assessment of the cytotoxicity of the modified BHA bioceramics. Long-term contact of the material with the cells (48 h) and low impact on their viability indicates a high potential for the use of these composites to create non-toxic materials for medical purposes.

## Conclusions

Biogenic hydroxyapatite bioceramics modified by graphene-like structures were prepared by chemical vapor deposition (CVD) method. The formation of graphene-like structures on the surface of silicon single crystals and biogenic hydroxyapatite using CVD method was confirmed by XRD,

IR spectroscopy and Raman techniques. SEM also showed coating formation and decreasing of specific surface area. According to investigation materials in vitro, it was established that modification BHA by graphene-like structures allows to 4 times increase resorption rate of BHA bioceramics in physiological solution. Moreover, long-term contact of the material with the cells (48 h) shows non-cytotoxic effect of BHA-GO bioceramics.

**Funding** This research work contains the results obtained according to the research project No. UMO-2022/01/3/ST5/00050 funded by the National Science Center within special program for scientists from Ukraine to continue their research in Poland.

**Data availability** The data can be openly available.

## Declarations

**Conflict of interest** The authors declare that there are no conflicts of interest regarding the publication of this manuscript.



## References

Arokiasamy P, Abdullah MMAB, Abd Rahim SZ et al (2022) Synthesis methods of hydroxyapatite from natural sources: a review. Ceram Int 48:14959–14979. https://doi.org/10.1016/j.ceramint.2022.03.064

Chandra Sekhar Boyapati P, Srinivas K, Akhil S (2022) Green synthesized graphene-hydroxyapatite nanocomposites for bioimplant applications. Mater Lett 327:133059. https://doi.org/10.1016/j.matlet.2022.133059

Claramunt S, Varea A, López-Díaz D et al (2015) The importance of interbands on the interpretation of the Raman spectrum of graphene oxide. J Phys Chem C 119:10123–10129. https://doi.org/10.1021/acs.jpcc.5b01590

Ghosal K, Mondal P, Bera S et al (2021) Graphene family nanomaterials- opportunities and challenges in tissue engineering applications. New J 30:100315. https://doi.org/10.1016/j.flatc.2021.100315. (**we have not received input yet**)

Gregg SJ, Sing KSW (1982) Adsorption, Surface Area and Porosity, 2nd edn. Academic Press, London

Heise U, Osborn JF, Duwe F (1990) Hydroxyapatite ceramic as a bone substitute. Int Orthop 14:329–338. https://doi.org/10.1007/bf00178768

Hench L, Jones J (2005) Biomaterials, artificial organs and tissue engineering. Woodhead Publishing Series in Biomaterials, Kidlington

Kaniyoor A, Ramaprabhu S (2012) A Raman spectroscopic investigation of graphite oxide derived graphene. AIP Adv 2:032183. https://doi.org/10.1063/1.4756995

Kattimani VS, Kondaka S, Lingamaneni KP (2016) Hydroxyapatite—past, present, and future in bone regeneration. Bone Tissue Regen Insights 7:9–19. https://doi.org/10.4137/BTRI.S36138

Li M, Xiong P, Yan F et al (2018) An overview of graphene-based hydroxyapatite composites for orthopedic applications. Bioact Mater 3:1–18. https://doi.org/10.1016/j.bioactmat.2018.01.001

Mc Naught AD, Wilkinson A (2019) Compendium of chemical terminology. IUPAC recommendations, 2nd edn. Academic Press, New York

Panchenko LM, Sych EE, Yatsenko AP (2014) The efficiency of cloning stem stromal cells of the human bone marrow in the presence of highly porous glass-ceramics and its solubility ex vivo. Vist Ortoped Travmatol Profitez 4:50–55

Sadat-Shojai M, Khorasani M-T, Dinpanah-Khoshdargi E et al (2013) Synthesis methods for nanosized hydroxyapatite with diverse structures. Acta Biomater 9:7591–7621. https://doi.org/10.1016/j.actbio.2013.04.012

Shi H, Zhou Z, Li W et al (2021) Hydroxyapatite based materials for bone tissue engineering: a brief and comprehensive introduction. Crystals 1:149. https://doi.org/10.3390/cryst11020149

Slobodian OM, Lytvyn PM, Nikonenko AS et al (2018) Low-temperature reduction of graphene oxide: electrical conductance and scanning kelvin probe force microscopy. Nanoscale Res Lett 13:139. https://doi.org/10.1186/s11671-018-2536-z

Sych EE (2015) Effect of pyrogenic silicon dioxide on the structure and properties of hydroxyapatite based bioceramics. Glass Ceram 72:107–110. https://doi.org/10.1007/s10717-015-9735-1

Sych O, Pinchuk N (2007) Effect of type of calcium phosphate on microstructure and properties of glass reinforced biocomposites. Process Appl Ceram 1:1–4

Sych O, Pinchuk N, Parkhomey A et al (2007) Morphology and properties of new porous biocomposites based on biogenic hydroxyapatite and synthetic calcium phosphates. Funct Mater 14:430–435

Sych O, Pinchuk N, Klymenko V et al (2015) Si-modified BHA bioceramics as a drug delivery system: effect of modification method on structure and Rifampicin release. Process Appl Ceram 9:125–129. https://doi.org/10.2298/PAC1503125S

Sych O, Gunduz O, Pinchuk N et al (2016) Tissue engineering scaffolds from $La_2O_3$-hydroxyapatite/boron glass composites. J Aust Ceram Soc 52:103–110

Sych O, Iatsenko A, Tovstonoh H (2017) Effect of fluorine addition on the structure and properties of high-porous glass ceramics applicable for reconstructive surgery. Funct Mater 24:46–51. https://doi.org/10.15407/fm24.01.046

Sych O, Iatsenko A, Tomila T et al (2018a) Si-modified highly-porous ceramics based on nanostructured biogenic hydroxyapatite for medical use. Adv Nano-Bio-Mater Devices 2:223–229

Sych OE, Iatsenko AP, Tomila TV (2018b) Effect of chitosan coating on the structure and properties of highly-porous bioceramic scaffolds for bone tissue engineering. Nanosistemi Nanomateriali Nanotehnologii 18:437–447. https://doi.org/10.15407/nnn.18.02.437

Tovstonog GB, Sych OE, Skorokhod VV (2015) The structure and properties of biogenic hydroxyapatite ceramics: microwave and conventional sintering. Powder Metall Met Ceram 53:566–573. https://doi.org/10.1007/s11106-015-9651-5

Tovstonoh HB, Panchenko LM, Sych OY (2016) Cloning efficiency of human bone marrow stem cells in the presence of hydroxyapatite ceramics prepared by microwave and traditional sintering. Trauma 17:45–49. https://doi.org/10.22141/1608-1706.4.17.2016.77488

Turk S, Altinsoy I, Efe GC et al (2018) The effect of reduction of graphene oxide on the formation of hydroxyapatite and tricalcium

phosphate. Vacuum 148:1–10. https://doi.org/10.1016/j.vacuum.2017.10.037
Zhang Y, Nayak TR, Hong H et al (2012) Graphene: a versatile nanoplatform for biomedical applications. Nanoscale 4:3833–3842. https://doi.org/10.1039/c2nr31040f
Zhang F, Yang K, Liu G et al (2022) Recent advances on graphene: synthesis, properties and applications. Compos Part A 160:107051. https://doi.org/10.1016/j.compositesa.2022.107051